Probing the Diffusion of a Dilute Dye Solution in Mesoporous Glass with Fluorescence Correlation Spectroscopy

S. M. Mahurin, Sheng Dai,* and M. D. Barnes

Chemical Sciences Division, Oak Ridge National Laboratory, Oak Ridge, Tennessee 37831

Received: July 14, 2003; In Final Form: October 8, 2003

The translational motion of rhodamine 6g dye molecules near the surface of a mesoporous glass with a disordered pore structure and a nominal pore diameter of 130 Å is measured by the application of fluorescence correlation spectroscopy (FCS) to fluorescence burst data as dye molecules diffuse through the laser excitation volume. FCS analysis indicates that the motion of the rhodamine 6g molecules in the mesoporous glass deviates from simple Brownian motion with a single diffusion constant. Two models, including two-component diffusion and diffusion plus adsorption, are utilized to fit the correlation data. The multicomponent diffusion model comprised of free diffusion (with a diffusion coefficient of 4.89×10^{-7} cm^2/s) and transient adsorption/desorption (desorption time of 67 ms) provides the best fit and the most plausible explanation of the correlation data. Possible explanations for the shift to multicomponent diffusion, such as restriction of the dye molecules within the pores of the glass, as well as increased viscosity and adsorption at the surface, are presented.

Introduction

The ultrasensitive detection and characterization of single molecules represents one of the most important achievements in optical spectroscopy in the past decade with potential applications in a wide variety of research areas such as chemical separations, DNA analysis, biotechnology, and nanostructured materials.[1−5] Since the first nondestructive optical detection of single pentacene molecules in a *p*-terphenyl crystal host,[6,7] a number of technical improvements have allowed the identification and dynamic investigation of various single chromophores in a wide range of host materials including room-temperature liquids,[8−10] polymer gels,[11] channels,[12] surfaces,[13] and membranes.[14] The ability to perform measurements at the single molecule level is the ultimate limit in chemical analysis with many advantages over corresponding bulk spectroscopic measurements. For instance, measurements obtained at such high levels of sensitivity can substantially reduce sample volume requirements, which is crucial for the success of miniaturized analytical devices, a topic that has received considerable research attention. However, the primary advantage of operating in the single molecule regime lies in the elimination of ensemble averaging, which can often obscure important fundamental properties of the system that might remain hidden in a large population measurement. Fluorescence characteristics of individual molecules can also serve as sensitive probes of local environmental inhomogeneities in a host material or reveal conformational changes in large complex molecules such as proteins via small fluorescent probes preferentially attached to selected sites within the protein molecule. A number of techniques have been developed to probe the dynamic properties of single chromophore systems since the investigation of diffusing molecules can provide significant insight into the nature of a system. This is especially true in applications in the biosciences where single molecule tracking has been applied to real-time visualization of the infection pathways of viruses into living cells.[15] In addition, single particle tracking was recently employed to image single protein molecules diffusing within a cell nucleus, which is of particular importance in the fundamental understanding of proteins.[16] Fluorescence correlation spectroscopy, an alternative to single particle tracking in the study of diffusion processes, has experienced an increase in popularity due in part to single molecule sensitivity as well as simplicity of the measurement process.

Fluorescence correlation spectroscopy (FCS) was initially developed to probe the dynamics of DNA denaturation by monitoring the binding of ethidium bromide, which is a small dye molecule that becomes fluorescent upon intercalation into double-stranded DNA.[17,18] The technique has since proven to be extremely versatile not only as a means of quantifying the kinetics associated with a variety of chemical processes, but also as a method for observing translational diffusion and rotation of dilute species. FCS is essentially a statistical analytical method based on fluctuations in fluorescence intensity about a mean fluorescence intensity, $\langle F(t)\rangle$, that can reveal nonequilibrium characteristics of the system. These fluctuations, which can arise from changes in the local concentration as fluorophores diffuse through the sampling volume or from the formation of reaction products, are autocorrelated as a function of time thus revealing properties about the diffusion process or permitting the measurement of reaction kinetics. Mathematically, the autocorrelation step is accomplished by multiplying the fluorescence intensity measured at time t by the intensity measured at time $t + \tau$ and integrating the product over some period of time. The normalized autocorrelation function for a fluorescent species with a fluorescence intensity of $F(t)$ at time t is given by the following:

$$G(\tau) = \frac{\langle \delta F(t) \cdot \delta F(t+\tau) \rangle}{\langle F(t) \rangle^2} \qquad (1)$$

where $\delta F(t)$ corresponds to the intensity fluctuation at time t and $\delta F(t + \tau)$ is the intensity fluctuation at some later time. For a single fluorescent species undergoing Brownian diffusion, the autocorrelation function is the probability that a molecule

* Address correspondence to this author. Phone: 865-576-7307. Fax: 865-76-5235. E-mail: dais@ornl.gov.

10.1021/jp036033t CCC: $25.00
Published on Web 11/11/2003

in the laser volume at time t is in the laser volume at time $t + \tau$.

To reduce background fluorescence, FCS measurements are generally performed on small focal volumes on the order of 1 fL as defined by the laser focal spot and the detection optics. For a focused Gaussian beam, the observation volume in three dimensions takes the form of a prolate ellipsoid:

$$I(r) = I_0 \exp\left[\frac{-2(x^2 + y^2)}{r_0^2} - \frac{2z^2}{z_0^2}\right] \quad (2)$$

where r_0 is the beam radius (or lateral beam waist) and z_0 is the beam height in the axial direction. The autocorrelation function for a single fluorescent species diffusing through a three-dimensional Gaussian intensity profile is given by:

$$G(\tau) = \frac{1}{N}\left(1 + \frac{\tau}{\tau_D}\right)^{-1}\left(1 + \frac{\tau}{\omega^2\tau_D}\right)^{-1/2} \quad (3)$$

where τ is the time lag, $\omega = \{z_0\}/\{r_0\}$, N is the mean number of molecules, and τ_D is the characteristic diffusion time in which a probe molecule resides in the focal volume of the laser. The diffusion coefficient, D, is related to the characteristic diffusion time by $\tau_D = \{r_0^2\}/\{4D\}$. The mean number of fluorescent molecules, or molecular concentration, can be calculated from the initial correlation amplitude $G(0) = 1/N$. This inverse relationship between the correlation amplitude and the molecular concentration can be explained in an intuitive fashion by noting that as the number of fluorescent molecules in the observation volume increases the effect of one molecule on the total measured fluorescence decreases.

FCS has found extensive applicability in the investigation of single diffusing molecules. For example, Schwille and co-workers utilized both one-photon and two-photon fluorescence correlation spectroscopy measurements to investigate molecular dynamics within a living cell.[19] FCS was recently used to study the diffusion of humic substances, which are useful model environmental compounds and have applications in the binding and transport of pollutants in waterways.[20] The diffusion of single DiI-C_{12} molecules in cell membranes has been measured by FCS in which analysis of the correlation curves suggested the presence of either anomalous or multicomponent diffusion through the membranes.[14] Ludes and Wirth used FCS to study the rare adsorption of DiI at the chromatographic interface of a C_{18} monolayer on silica and acetonitrile/water.[21] With the current emphasis on nanoscale systems, the diffusion of single molecules through submicron channels is becoming increasingly important. Lyon and Nie investigated diffusion and flow through electrophoresis capillaries with a width of 500−600 nm and observed a reduction in the characteristic diffusion time as a result of size restrictions and electrostatic interactions with the silica walls.[12] Of particular interest is the application of FCS to the motion of single molecules in porous materials, which often serve as separation media or supports for catalysts.[22−28] Due to the size of the pores, mesoporous materials offer an excellent framework in which to observe motion under geometrical constraints and possibly gain a greater fundamental understanding of the effects of confinement and molecule−wall interactions on the diffusion process. A fairly recent experiment by Seebacher and co-workers showed that the motion of single terrylenediimide molecules cosynthesized in a mesostructured silica film by single particle tracking followed simple Brownian diffusion.[29] In this work, we employ fluorescence correlation spectroscopy to study the diffusion of single rhodamine 6g dye molecules in a high-temperature mesoporous glass with a nominal pore size of 130 Å with negligible micropores. We find that a two-component diffusion model is necessary to fit the measured correlation data.

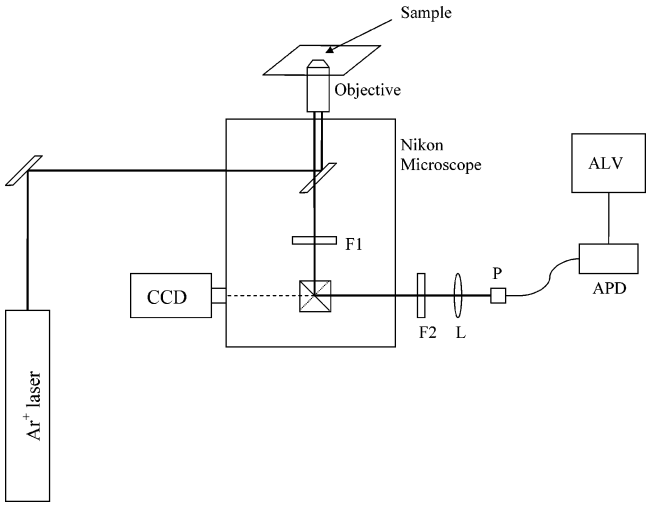

Figure 1. Schematic diagram of the experimental setup for measuring diffusion of single molecules. Light from an argon ion laser is directed into a high-NA objective to the sample. Fluorescence collected by the same objective goes through a long pass filter (F1) and can be sent to a CCD camera or through a band-pass filter (F2) where it is focused by a lens (L) into a pinhole (P) and optical fiber to the avalanche photodiode (APD). The correlator card (ALV) autocorrelates the data.

Experimental Section

The apparatus used for this experiment consisted of a Nikon TE2000 inverted microscope operating in epi-illumination mode (see Figure 1). The 514.5-nm line from an argon ion laser was used as the excitation source. An important consideration in single molecule experiments is the possible introduction of artifacts into the analysis due to photobleaching of the dye molecules as they traverse the observation volume at high laser powers. For this reason, the laser power was kept low (approximately 200 μW at the microscope objective) to avoid artificially reducing the diffusion time as a result of photobleaching. The laser entered the microscope through the back port after spatial filtering and was directed into a high numerical aperture oil immersion objective (Nikon 100×, 1.3 NA) by a dichroic mirror. The objective then focused the beam to a diffraction-limited spot. Fluorescence from the sample was collected by the same objective and was directed into either a CCD camera (MicroMax, Roper Scientific) for imaging or a high-efficiency avalanche photodiode (APD) for single photon counting and subsequent calculation of the correlation spectra. Since fluorescence correlation spectroscopy is based on fluctuations in the total fluorescence intensity, it is essential that background fluorescence be minimized. A long pass filter (Melles-Griot) with a cut-on wavelength at 550 nm and an interference band-pass filter (Omega Optical, Inc) were used to reduce background fluorescence. A 20× microscope objective (Newport) focused the fluorescence signal onto a 62.5 μm multimode optical fiber, which was used in place of a pinhole to effectively reject out-of-focus background fluorescence. The signal was then transmitted to an avalanche photodiode (Perkin-Elmer, SPCM-AQR-15) equipped with an optical fiber attachment for photon detection. The APD has a high detection efficiency and low dark count (∼50 cts/s) thus enabling the detection of single molecule events as they pass through the focal volume of the laser. The signal from the APD was then

sent to a correlator card (ALV-6010, ALV-Laser, Germany), which calculated the correlation function.

A sample cuvette was constructed by attaching a glass cylinder to a #1 glass coverslip with TorrSeal (Varian Vacuum Technologies). A rubber stopper was inserted into the top of the cuvette to prevent solvent evaporation during data collection. Semiconductor grade methanol and HPLC water were purchased from Sigma Aldrich and used without further purification. A solution of rhodamine 6g in methanol (5×10^{-11} M) was prepared by serial dilution of a stock solution prior to use. Since contaminants from the cuvette could potentially introduce errors into the FCS analysis, the sample cuvette was cleaned with concentrated detergent and rinsed extensively with water purified from a MilliQ water filter system (nominal resistance of $R \sim 17$ kΩ). The mesoporous glass samples (Advanced Glass and Ceramics) were heated at 700 °C for 2 h to remove any fluorescent contaminants that might interfere with the measured signal. The uniform pore size of this porous glass was verified by N_2-adsorption isotherm measurement before each experiment. Surface areas and pore volumes were measured on a Micromeritics Gas sorption system (Micromeritics Corp.). The BET surface area is 109 m^2/g and the total pore volume is 0.270 cm^3/g. The average mesopore diameter calculated with use of the Barrett−Joyner−Hallenda (BJH) method is 130 Å.[30]

Results and Discussion

Accurate evaluation of the correlation data to obtain information on the diffusing fluorophores requires a complete description of the focused beam spot since diffusion coefficients derived from FCS measurements are sensitive to the dimensions of the probe volume. In particular, parameters such as the beam radius, r_0, and height, z_0, must be precisely known to extract useful information from the measured correlation curves. In theory, a high-NA objective focuses a beam with a Gaussian intensity profile to a diffraction-limited spot with a lateral radius on the order of the illumination wavelength ($r_0 \sim 0.5$ μm with a corresponding beam height of $z_0 = 1.53$ μm). However, in practice, theoretical beam dimensions are often not achieved due to optical effects such as spherical aberration. Because beam dimensions are not easily obtained directly, calibration of the system, i.e., determination of both the beam radius and height of the probe volume, was accomplished by evaluating the diffusion of Rh6g in water, which has a known diffusion coefficient of 2.8×10^{-6} cm^2/s.[31] One-hundred microliters of a Rh6g solution (5×10^{-11} M) was pipetted into the sample cuvette and a series of four correlation curves were acquired. The autocorrelation curves were then fit to eq 3 by using a Levenberg−Marquardt χ^2 minimization procedure within Microcal Origin to obtain the relevant beam dimensions, $r_0 = 0.650$ μm and $z_0 = 2.58$ μm. The four measurements yielded an average diffusion coefficient of $(2.81 \pm 0.16) \times 10^{-6}$ cm^2/s, which is in excellent agreement with the known value. On the basis of the measured beam dimensions, the probe volume is estimated to be ~4 fL.

Typically, the mesoporous glass was placed into the cuvette partially filled with dye solution. Due to surface roughness in the mesoporous glass, the separation between the coverslip and the glass was approximately 30 μm. Thus, to measure the diffusion coefficient within the glass, it was necessary to focus the beam as well as detect the emitted fluorescence through a refractive index mismatch between the glass coverslip and the Rh6g in methanol solution. This refractive index mismatch can reduce the overall collection efficiency of the objective and cause changes in the shape of the laser beam, which could ultimately lead to errors in the measured diffusion coefficient.

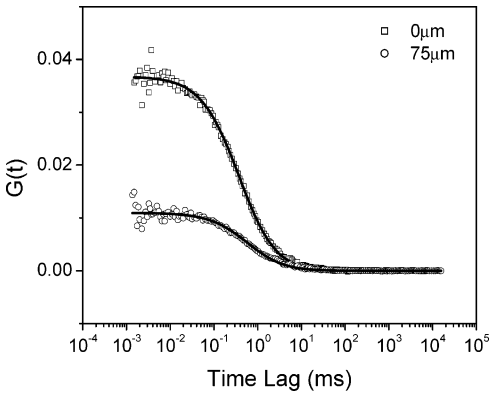

Figure 2. Correlation curves acquired at the surface of the coverslip, which corresponds to $z = 0$ μm, and at $z = 75$ μm. The decrease in the correlation amplitude is due to the increase in the background at greater depth within the solution.

We examined this issue by acquiring correlation spectra for Rh6g in methanol (no mesoporous glass) at various z positions, where z indicates the height above the coverslip and $z = 0$ corresponds to the surface of the coverslip. Figure 2 shows correlation spectra taken at two z positions, $z = 0$ and 75 μm. The most obvious effect of z position on the measured correlation curves is the observed decrease in the correlation amplitude $G(0)$, which is primarily due to an increase in the background fluorescence at higher z position and leads to an increase in the calculated molecular concentration. It is also important to realize that simple Brownian motion with a single diffusion coefficient remains adequate to explain the motion of the dye molecules even at large z positions as confirmed by the excellent fit between the correlation data and the model. To further explore the z dependence, correlation curves were acquired and analyzed at 10-μm intervals above the coverslip (see Figure 3). The diffusion coefficient decreased from an initial value of 2.81×10^{-6} cm^2/s at $z = 0$ to a lower limit of 1.66×10^{-6} cm^2/s, while the molecular concentration showed a linear increase from 27 to 108 molecules/focal volume. In a recent paper on the diffusion of a rhodamine dye in a planar phospholipid system, Benda and co-workers observed a similar dependence of diffusion coefficient and molecular concentration on the z-position.[32] However, in that work, only a small range of z (~2 μm) was investigated. Thus, while the measured diffusion coefficient is influenced by the z position, the effect can be taken into account when measurements are made within the mesoporous glass.

In a typical experiment, 200 μL of the 5×10^{-11} M Rh6g in methanol solution was first pipetted into the cuvette, then the 130Å mesoporous glass was immersed in the dye solution. After allowing the system to equilibrate for ~5 min, correlation spectra were recorded at various z positions. Assuming a single species diffusing with uniform Brownian motion failed to produce an adequate fit to the correlation data as can be clearly seen in Figure 4a. We note, however, that the autocorrelation function can be extended to a single species with multiple diffusion coefficients by simply summing the contributions of each component. For a single chromophore with two diffusion coefficients, the multicomponent model has the following form:

$$G(\tau) = \frac{1}{N}\left\{P\left(1+\frac{\tau}{\tau_{D_1}}\right)^{-1}\left(1+\frac{\tau}{w^2\tau_{D_1}}\right)^{-1/2} + (1-P)\left(1+\frac{\tau}{\tau_{D_2}}\right)^{-1}\left(1+\frac{\tau}{w^2\tau_{D_2}}\right)^{-1/2}\right\} \quad (4)$$

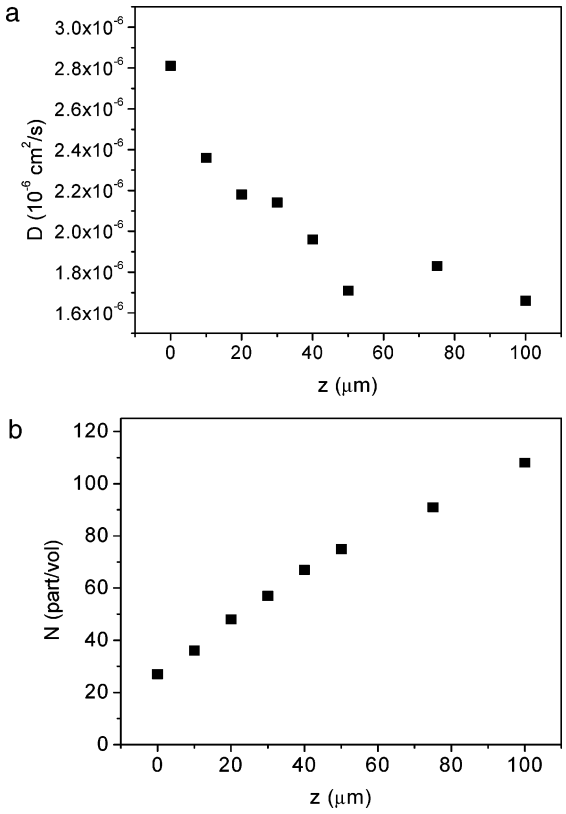

Figure 3. Graph of (a) the diffusion coefficient and (b) the molecular concentration, *N*, from FCS analysis as a function of the *z* position in the Rh6g solution.

where τ_{D_1} and τ_{D_2} are the two characteristic diffusion times, *P* is the probability that the molecule has diffusion coefficient τ_{D_1}, and *N* is the molecular concentration. Figure 4b, which gives the correlation spectrum fitted with a two-component model, illustrates that the two-component model provides a better fit to the correlation data than the single-component model. Analysis of correlation curves acquired at $z = 40$ μm, which corresponds to a distance of 10 μm into the mesoporous glass, yielded 38% of the particles with diffusion coefficient $D_1 = 6.81 \times 10^{-7}$ cm^2/s and 62% of the particles with $D_2 = 4.84 \times 10^{-8}$ cm^2/s. The majority of the molecules shifted to the slowest diffusion coefficient, possibly as a result of multiple contacts with the pore walls. The two-component diffusion exhibited by the dye molecules could be due to the disordered nature of the mesoporous structure, which leads to a more complex translational behavior. One surprising result appeared in the separation region between the coverslip and the mesoporous glass where motion was expected to be primarily single-component diffusion since this is a region of essentially free dye in solution. However, even in this separation region, a two-component model was required to properly fit the correlation data. Specifically, at the surface of the coverslip ($z = 0$ μm) correlation analysis revealed 60% of particles with $D_1 = 1.21 \times 10^{-6}$ cm^2/s and 40% of particles with $D_2 = 8.38 \times 10^{-8}$ cm^2/s.

Another possibility that would explain the behavior of the dye solution within the mesoporous glass as well as in the region between the glass and the coverslip is that the dye molecules undergo two distinct processes, specifically single-component diffusion and reversible adsorption/desorption. Wirth et al. have derived the autocorrelation function given below that describes systems undergoing free diffusion and rare strong adsorption/

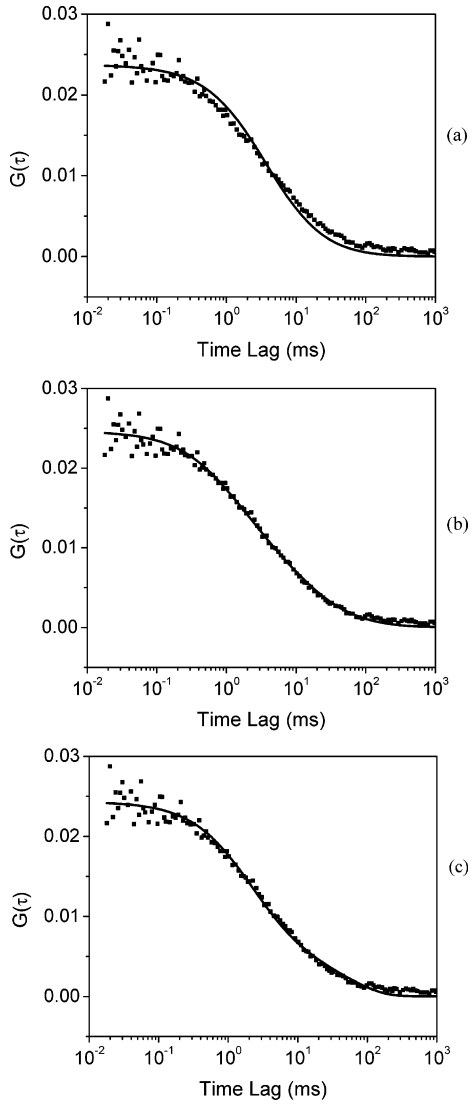

Figure 4. Correlation curve of Rh6g in mesoporous glass fitted with (a) a single diffusion coefficient, (b) two diffusion coefficients, and (c) a combination diffusion/adsorption model.

desorption:[33]

$$G(\tau) = \frac{1}{N}\left\{P\left(1+\frac{\tau}{\tau_{D_1}}\right)^{-1}\left(1+\frac{\tau}{w^2\tau_{D_1}}\right)^{-1/2} + (1-P)\exp\left[\frac{-\tau}{\tau_{D_2}}\right]\right\} \quad (5)$$

where *P* is the probability that the molecule undergoes free diffusion, and τ_{D_1} and τ_{D_2} are the diffusion times for free diffusion and adsorption, respectively. Figure 4c gives the correlation data with the diffusion plus rare strong adsorption fitting model. The diffusion/adsorption model fits the data as well as the two-component model and analysis yielded approximately 80% of the molecules undergoing free diffusion with a diffusion coefficient of $D_1 = 4.89 \times 10^{-7}$ cm^2/s and 20% of the molecules undergoing adsorption/desorption with a desorption time of 67 ms. While both the two-component and diffusion plus adsorption models fit the correlation data, the diffusion plus adsorption model is perhaps the more plausible one since the Rh6g probe has the opposite charge as the glass surface and it is necessary to adjust the model in the region between the glass and the coverslip. The signal-to-noise ratio was not sufficient to observe bursts from the adsorbed molecules

directly, which would have provided direct evidence to support the diffusion plus adsorption model.

While there is a definite shift in the mobility of the probe molecules to multicomponent diffusion, the magnitude of the shift seems insufficient to attribute the motion to diffusion through 130 Å pores. Though direct comparisons to previous work are difficult due to differences in experimental conditions, it is nonetheless instructive to note that research by Lyon and Nie on single molecules diffusing through 500-nm capillaries showed a reduction of nearly 2 orders of magnitude in the diffusion coefficient, which is comparable to the value that we obtained.[12] Moreover, mobile terrylenediimide molecules co-synthesized in a mesoporous silica host exhibited a single diffusion coefficient of 3.72×10^{-10} cm^2/s, which is significantly smaller than the diffusion coefficient measured in our experiment.[29] One possible explanation of the much slower diffusion in the mesoporous silica is that the silica was synthesized with use of a room-temperature sol−gel process that produces a large number of micropores in the film. These micropores tend to increase the surface roughness of the pore walls as well as provide additional interaction sites for the diffusing molecules, which would further decrease the diffusion coefficient. The high-temperature glass used in our experiments did not possess these micropores, as indicated by BET measurements. This lack of surface roughness and interaction sites could contribute to the higher diffusion coefficient measured in our experiment. In addition to the somewhat high diffusion coefficient, the necessity of the multicomponent diffusion model even near the coverslip ($z = 0\ \mu$m) suggests possible adsorption effects in the separation region between the mesoporous glass and the coverslip, or potential artifacts introduced by the mesoporous glass. To check for potential artifacts, the experiment was repeated with a 1 cm × 1 cm section of coverslip in place of the mesoporous glass with a resulting separation region of 25 μm. In this case, a single diffusion coefficient was sufficient to properly fit the correlation data throughout the separation region, while the dependence of the measured diffusion coefficient on the z position was similar to the free dye case indicating that simply the presence of an immersed sample, e.g. the coverslip or the glass sample, does not alter the type of diffusion.

Brightfield optical images of the mesoporous glass surface revealed an extremely irregular surface marked by numerous micron-size corrugations and protrusions. Thus the shift to diffusion plus adsorption in the separation region might be attributed to the presence of these microchannels at the surface of the mesoporous glass, some of which extend to the surface of the coverslip and provide numerous sites for specific adsorption of the Rh6g. It should be noted that the glass sample is a high-temperature glass with relatively few silanol groups on the surface for the mobile dye molecules to interact with. These silanol groups would tend to reduce the diffusion coefficient of the probe species even further, particularly in the framework of micron and submicron confinement. However, in the case of the high-temperature glass, these surface effects should be minimal.

Conclusion

We have demonstrated the use of fluorescence correlation spectroscopy in the analysis of molecules diffusing through a porous glass material with a variety of surface irregularities and channels. Rhodamine 6g probe molecules diffusing within the mesoporous glass sample experienced a shift to a multicomponent diffusion model comprised of free diffusion and transient adsorption with an overall decrease in the diffusion coefficients. Reduction of the diffusion coefficient is primarily due to multiple contacts of the single analyte molecules with the walls rather than interactions with functional groups on the surface of the mesoporous glass, which are expected to be minimal since the sample is a high-temperature glass. The two-component model observed in the separation region could be attributed to adsorption of the dye molecules along the roughened surface of the mesoporous glass. Experiments are currently underway to further investigate diffusion in mesoporous materials, specifically in thin films deposited onto the coverslip where significant reduction in any artifacts that might be introduced as a result of measurements obtained through a refractive index mismatch is expected.

Acknowledgment. This work was conducted at the Oak Ridge National Laboratory and supported by the Office of Basic Energy Sciences, U.S. Department of Energy (DOE), under contract No. DE-AC05-00OR22725 with UT-Battelle, LLC. This research was supported in part by an appointment for S.M.M. to the ORNL Research Associates Program, administered jointly by ORNL and the Oak Ridge Institute for Science and Education. The authors thank Dr. Zuojiang Li for performing BET measurements and a reviewer for helpful suggestions.

References and Notes

(1) Moerner, W. E. *Science* **1994**, *265*, 46.
(2) Wang, H.; Bardo, A. M.; Collinson, M. M.; Higgins, D. A. *J. Phys. Chem. B* **1998**, *102*, 7231.
(3) Hess, S. T.; Huang, S.; Heikal, A. A.; Webb, W. W. *Biochemistry* **2002**, *41*, 697.
(4) Fister, J. C.; Jacobson, S. C.; Davis, L. M.; Ramsey, J. M. *Anal. Chem.* **1998**, 70, 431.
(5) Eigen, M.; Rigler, R. *Proc. Natl. Acad. Sci. U.S.A.* **1994**, *91*, 5740.
(6) Moerner, W. E.; Kador, J. *Phys. Rev. Lett.* **1989**, *62*, 2535.
(7) Orrit, M.; Bernard, J. *Phys. Rev. Lett.* **1990,** *65*, 2716.
(8) Barnes, M. D.; Whitten, W. B.; Ramsey, J. M. *Anal. Chem.* **1995**, *67*, 418A.
(9) Nie, S.; Chiu, D. T.; Zare, R. N. *Anal. Chem.* **1995**, *67*, 2849.
(10) Betzig, E.; Chichester, R. J. *Science* **1993**, *262*, 1422.
(11) Dickson, R. M.; Norris, D. J.; Tzeng, Y.-L.; Moerner, W. E. *Science* **1996**, *274*, 966.
(12) Lyon, W. A.; Nie, S. *Anal. Chem.* **1997**, *69*, 3400.
(13) Hanley, D. C.; Harris, J. M. *Anal. Chem.* **2001**, *73*, 5030.
(14) Schwille, P.; Korlach, J.; Webb, W. W. *Cytometry* **1999**, *36*, 176.
(15) Seisenberger, G.; Ried, M. U.; Endreb, T.; Büning, H.; Hallek, M.; Bräuchle, C. *Science* **2001**, *294*, 1929.
(16) Kues, T.; Peters, R.; Kubitscheck, U. *Biophys. J.* **2001**, *80,* 2954.
(17) Magde, D.; Elson, E.; Webb, W. W. *Phys. Rev. Lett.* **1972**, *29*, 705.
(18) Elson, E. L.; Magde, D. *Biopolymers* **1974**, *13*, 1.
(19) Schwille, P.; Haupts, U.; Maiti, S.; Webb, W. W. *Biophys. J.* **1999**, *77*, 2251.
(20) Lead, J. R.; Starchev, K.; Wilkinson, K. J. *Environ. Sci. Technol.* **2003**, *37*, 482.
(21) Ludes, M. D.; Wirth, M. J. *Anal. Chem.* **2002**, *74*, 386.
(22) Kresge, C. T.; Leonowicz, M. E.; Roth, W. J.; Vartuli, J. C.; Beck, J. S. *Nature* **1992**, *359*, 710.
(23) Corma, A. *Chem. Rev.* **1997**, *97*, 2373.
(24) Davis, M. E. *Nature* **2002**, *417*, 813.
(25) Stein, A. *Adv. Mater.* **2003**, *15*, 763.
(26) Feng, X.; Fryxell, G. E.; Wang, L. Q.; Kim, A. Y.; Liu, J.; Kemner, K. M. *Science* **1997**, *276*, 923.
(27) Dai, S.; Burleigh, M. C.; Shin, Y. S.; Morrow, C. C.; Barnes, C. E.; Xue, Z. L. *Angew. Chem., Int. Ed.* **1999**, *38*, 1235.
(28) Dai, S.; Burleigh, M. C.; Ju, Y. H.; Gao, H. J.; Lin, J. S.; Pennycook, S.; Barnes, C. E.; Xue, Z. L. *J. Am. Chem. Soc.* **2000**, *122*, 992.
(29) Seebacher, C.; Hellriegel, C.; Deeg, F.; Bräuchle, C.; Altmaier, S.; Behrens, P.; Müllen, K. *J. Phys. Chem. B* **2002**, *106*, 5591.
(30) Barret, E. P.; Joyner, L. G.; Hallenda, P. P. *J. Am. Chem. Soc.* **1951**, *73*, 373.
(31) Rigler, R.; Mets, U.; Widengren, J.; Kask, P. *Eur. Biophys. J.* **1993**, *22*, 169.
(32) Benda, A.; Beneš, M.; Marecek, V.; Lhotsky, A.; Hermens, W. Th.; Hof, M. *Langmuir* **2003**, *19*, 4120.
(33) Wirth, M. J.; Ludes, M. D.; Swinton, D. J. *Appl. Spectrosc.* **2001**, *55* (6), 663.